INVESTIGATION OF GAMMA RADIATION SHIELDING FEATURES FOR MODIFIED STRUCTURAL MATERIALS FOR NUCLEAR ENERGY AND NUCLEAR MEDICINE

by

***Yuliya ZARIPOVA* [1*], *Vyacheslav DYACHKOV* [1], *Tatyana GLADKIKH* [2], *Mirgul BIGELDIYEVA* [1], *and Nasr Ahmed Nasr DIAB* [3]**

[1] Faculty of Physics and Technology, Al-Farabi Kazakh National University, Almaty, Kazakhstan
[2] Suncar Medical Center, Almaty, Kazakhstan
[3] Cairo University, Giza, Egypt

Scientific paper
https://doi.org/10.2298/NTRP2302108Z

In this paper, shielding characteristics of three concrete samples with different B_4C, Fe_3O_4, and $BaSO_4$ contents were examined by determining their theoretical and experimental mass attenuation coefficients at photon energies of 15 MeV. The mass attenuation coefficients μ_m were theoretically calculated using the chemical compositions of samples with the XCOM program. Then the linear attenuation coefficients μ were calculated by knowing the μ_m values. Elekta Axesse accelerator was used to experimentally determine the linear attenuation coefficients μ of samples with various impurities. The μ value of 0.4699 cm^{-1}, 0.6072 cm^{-1}, and 0.7194 cm^{-1} was obtained for the blank sample, sample with magnetite, and sample with barite, respectively, at 15 MeV. The results were compared with coefficients obtained by XCOM and indicated a good agreement between the two methods. The linear attenuation coefficient was evaluated to calculate the half- and tenth-value layers. Compared to conventional concrete, the linear attenuation coefficient for concrete with the highest barite content increased by 53.1 %, and the thickness of the half-attenuation layer decreased by 34.7 %. Such a sample can be used as a building material for medical centers and nuclear power plants.

Key words: concrete, radiation protection, linear attenuation coefficient, half-value layer

INTRODUCTION

Ensuring radiation protection is a key factor hindering progress in working with sources of radioactive radiation in many areas: medical physics [1, 2], dosimetry and radiation protection [3, 4], industry and technology [5-7], and radiation biophysics [8, 9]. The energy crisis is currently one of the pressing global problems. The burning of fossil fuels to generate electricity is no longer able to keep up with the demanded volume of consumption, and, in addition, the accompanying emissions of CO_2 into the atmosphere are one of the main causes of global climate change on Earth. One of the solutions to this problem is the use of a highly efficient resource – nuclear energy. World statistics show that 13 % of the electricity is produced by nuclear reactors, and in countries such as France and Sweden, this percentage more than doubles [10]. The use and development of this resource in other countries is constrained by the safety factor in the operation of nuclear reactors. As a new source of carbon-free base electricity that does not produce long-lived radioactive waste, fusion can make a positive contribution to resource availability, carbon reduction, fission waste disposal, and safety issues. During the construction of medical institutions that planned to use modern diagnostic and therapeutic equipment with sources of radioactive radiation, it is also necessary to account for building materials' physical and mechanical properties and their radiation-protective properties. As a rule, materials with high atomic numbers have the best shielding ability. Lead, iron, and materials containing these elements are good radiation shields. However, the use of only these materials in the construction of buildings due to their high cost is impossible. In addition, lead is toxic to humans and the environment, making it less than ideal as a building material. Therefore, less effective but cheaper shielding materials, such as sand, brick, cement, and concrete, are mainly used. By changing the composition of these materials, it is possible to increase their ability to attenuate radiation [11, 5].

Today, concrete is widely used for radiation protection: it is cheap, easy to form structures of various

* Corresponding author, e-mail: zjkaznu2016@gmail.com

shapes, and a good absorber [12, 13]. Radiation-protective concrete is a composite with special fillers. It is widely used for shielding against gamma-rays and neutrons due to its good shielding properties and is the biological barrier of choice in nuclear reactors and other nuclear installations. Various authors carried out studies to determine the attenuation coefficients for multiple materials, such as polymer composites [14, 15], alloys [16], glasses [17, 18], and concretes [19, 20]. Concrete was studied mainly at energies from 662 keV to 1332 keV [21-24]. However, despite this, the process of radiation damage to cement, which is part of concrete, and the effect of different concentrations of chemical elements on its radiation resistance are still insufficiently studied. Therefore, the study of materials used to provide effective radiation protection is an important area.

This work aimed to study concrete samples with different contents of B_4C, Fe_3O_4, and $BaSO_4$ to test their radiation resistance and sorption properties to optimize the design of protective materials at a gamma-quantum energy of 15 MeV. These energies are of interest for constructing optimal radiation protection in nuclear medicine centers and at future thermonuclear power engineering stations. Above the point of 10 MeV, a significant contribution is made by the processes of interaction of photons directly with the nucleus, that is, photonuclear reactions begin to occur. Accordingly, not considering high-energy gamma-rays will significantly underestimate the risk for both personnel and patients. A comparison of different concrete samples was carried out with a focus on the study of linear attenuation coefficients in the field of protection against gamma radiation.

MATERIAL AND METHODS

The studied concrete samples were made at Cairo University, Egypt. The composition and geometric characteristics of the samples are shown in tab. 1.

Fresh commercial ordinary (Type-I) Portland cement was used. Chemical analysis is shown in tab. 2.

Table 1. Mix for radiation shielding

Sample description		Blank sample (BS)	Sample 1 with magnetite (S1)	Sample 2 with barite (S2)
Composition [%]	Cement	30	30	30
	Sand	70	0	0
	Boron carbide	0	15	15
	Barite	0	0	55
	Magnetite	0	55	0
SBR latex [%]		10	10	10
Water to cement ratio		0.28	0.28	0.28
Density [gcm^{-3}]		2.3	2.7	2.8
Dimensions		2 cm × 10 cm × 10 cm		

Table 2. Cement composition

Compound	Weight [%]
SiO_2	20.33
$A1_2O_3$	4.20
Fe_2O_3	3.76
CaO	68.16
MgO	1.13
SO_3	1.37
Free $Ca(OH)_2$	1.1
Loss on ignition	2.2

The linear absorption coefficients of gamma-rays were studied at the Elekta Axesse electron accelerator [25] at an energy of 15 MeV. The choice of this energy is because: as a result of the deuterium-tritium (DT) reaction, high-energy gamma quanta are emitted, fig. 1 and as a result of radiation therapy in rooms with a medical linear accelerator, the following types of radiation are formed, fig. 2:

– primary beam – high-energy gamma quanta with energies up to 30 MeV, directed to the isocenter of the linear accelerator (gantry rotation point), which means that when using the rotational technique, this beam can fall on four of the six walls of the cabinets;

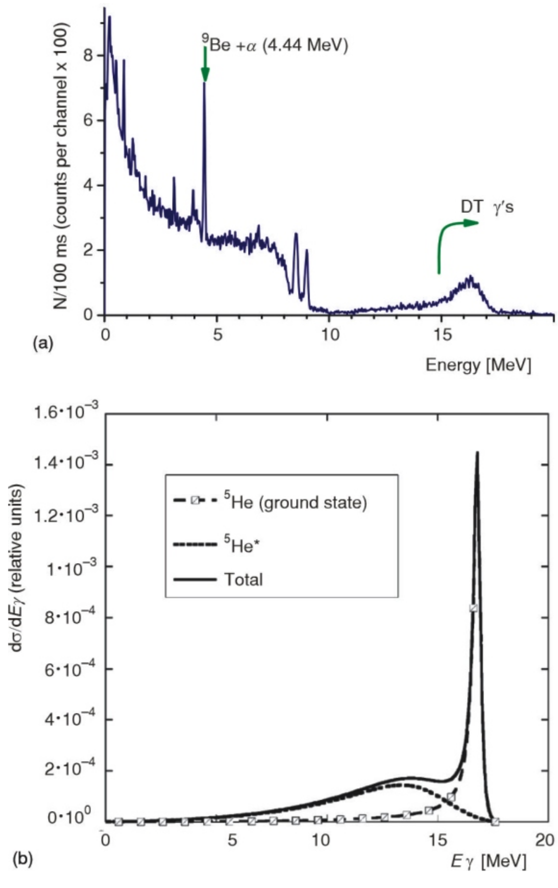

Figure 1. Gamma-ray spectrum; (a) which could be measured from ITER DT plasmas (500 MW) – MCNP calculations [26]; b) theoretical spectrum for the deuterium-tritium fusion reaction [27]

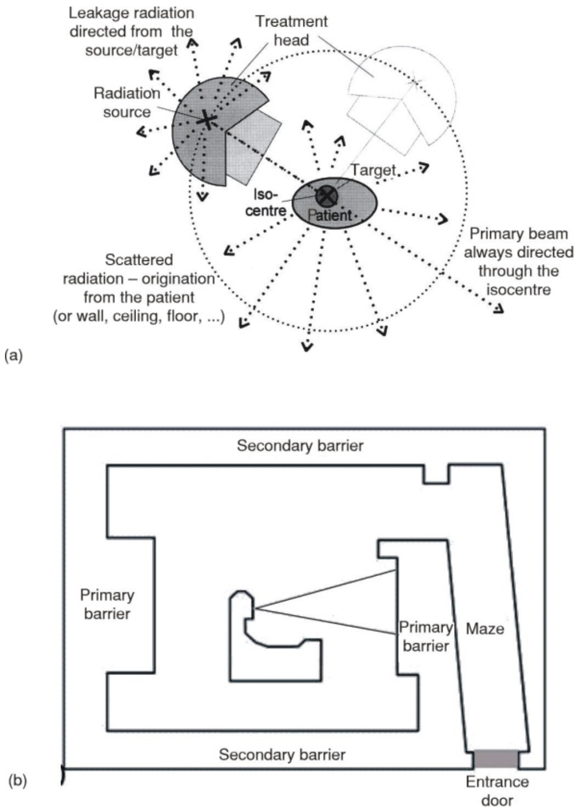

Figure 2. (a) Scheme of radiation of various types in the room of a linear accelerator and (b) scheme of typical radiotherapy treatment vault [28]

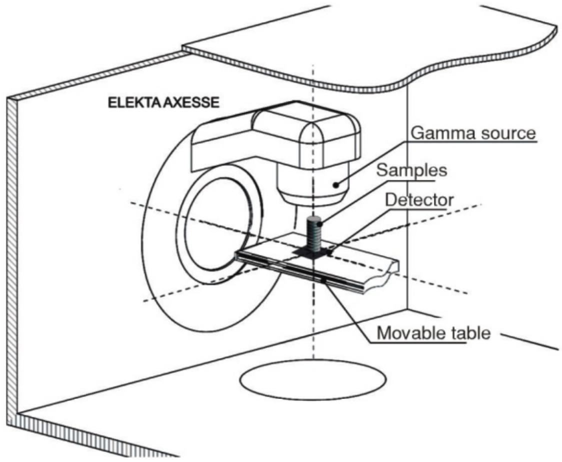

Figure 3. Scheme of the general view of the experiment with the electron accelerator Elekta Axesse

– scattered radiation emanating from the patient's body, the head of the linear accelerator, the walls of the room, and equipment, directed at a right solid angle, with a wide energy range [28].

The measurements were carried out in a laboratory located based of the Sunkar Medical Center (Almaty, Kazakhstan). Figure 3 shows a diagram of the general view of the experiment, which indicates the placement of the detector and samples on the movable table on the axis of the gamma-ray beam. Figure 4 shows photographs of the experiments on irradiating samples with gamma quanta.

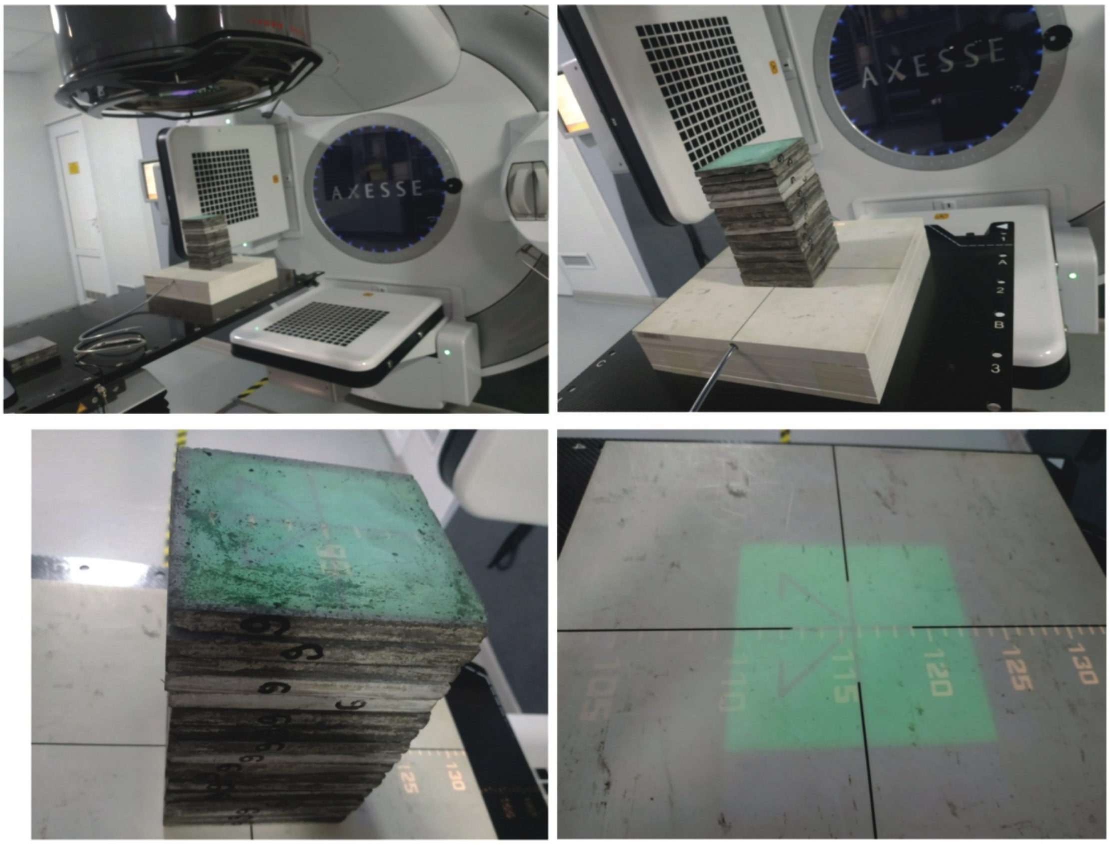

Figure 4. Samples on the movable stage of the Elekta Axesse electron accelerator

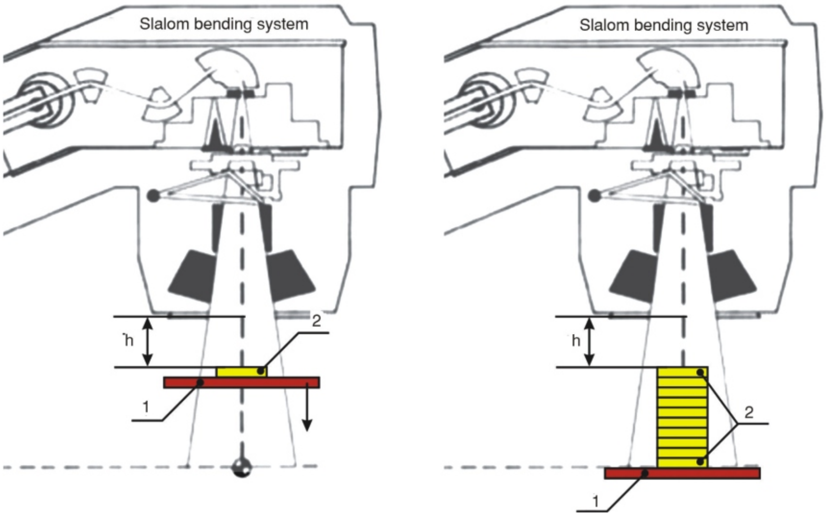

Figure 5. Scheme and geometry of measurements

Linear absorption coefficients for three concrete samples with different B_4C, Fe_3O_4, and $BaSO_4$ contents were obtained. A new technique for measuring linear attenuation coefficients at a linear medical accelerator was proposed and tested in [29]. The scheme and geometry of the measurement method are shown in fig. 5. To measure the absorbed dose of the gamma-ray beam, the detector was placed on a movable table and moved with an increase in the thickness of the test sample and by the corresponding value equal to 2 cm. Thus, the air gap thickness *h* between the sample under study and the source of gamma rays remained constant and was equal to 95 cm.

The recording system consisted of a Vented parallel ion chamber detector with an active measurement area of 24.4 cm × 24.4 cm, in which 1020 sensors were located, arranged in a 32 × 32 grid except for the four corner positions. Nominal sensitivity – 2.4 $nCGy^{-1}$. Dose Rate Dependence 1.0 % [25]. The profile of the beam obtained using the standard software package of the electron accelerator is shown in fig. 6.

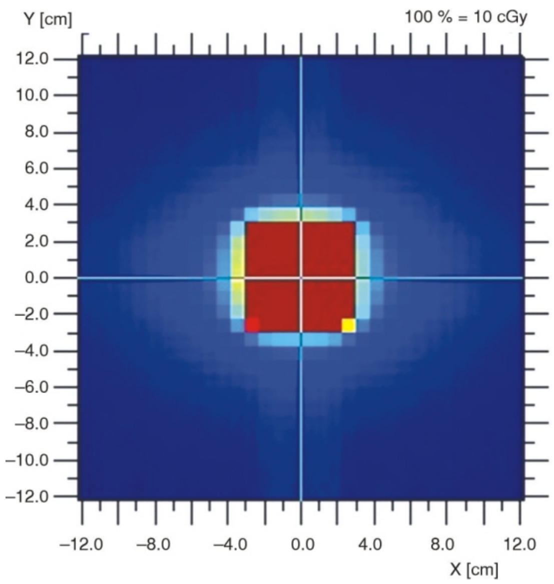

Figure 6. Gamma beam profile

To compare the experimental data, the samples' mass attenuation coefficients μ_m were also theoretically calculated using the XCOM program developed by Berger *et al*. [30]. The program calculates the mass attenuation coefficients depending on the chemical composition of the materials.

The linear gamma attenuation coefficients were calculated using eq. (1), and the mean free path (MFP), half-value layer (HVL), and tenth-value layer (TVL) were determined using eqs. (2)-(4) respectively [11]

$$\mu \quad \mu_m \gamma \tag{1}$$

$$\text{MFP} \quad \frac{1}{\mu} \tag{2}$$

$$\text{HVL} \quad \frac{\ln 2}{\mu} \tag{3}$$

$$TVL \quad \frac{\ln 10}{\mu} \tag{4}$$

where μ [cm^{-1}] is the linear attenuation coefficient, μ_m [cm^2g^{-1}] – the mass attenuation coefficient, and γ [gcm^{-3}] – the concrete density.

RESULTS AND DISCUSSION

The theoretical total mass attenuation coefficients are shown in fig. 7 for gamma-ray energies in the range from 0.001 to 10,000 MeV. Introducing barite into concrete samples increased the overall gamma attenuation coefficients below 0.5 MeV and above 5 MeV. This is most likely due to pair formation and the photoelectric effect, which can arise with an increase in the atomic number of a substance [31]. The theoretically calculated mass attenuation coefficients of the studied samples at a gamma-ray energy E_γ of 15 MeV are 0.02149, 0.02364, 0.02695 cm^2g^{-1} for the blank sample (BS), sample with magnetite (S1), and sample with barite (S2) samples, respectively. The model with barite (S2)

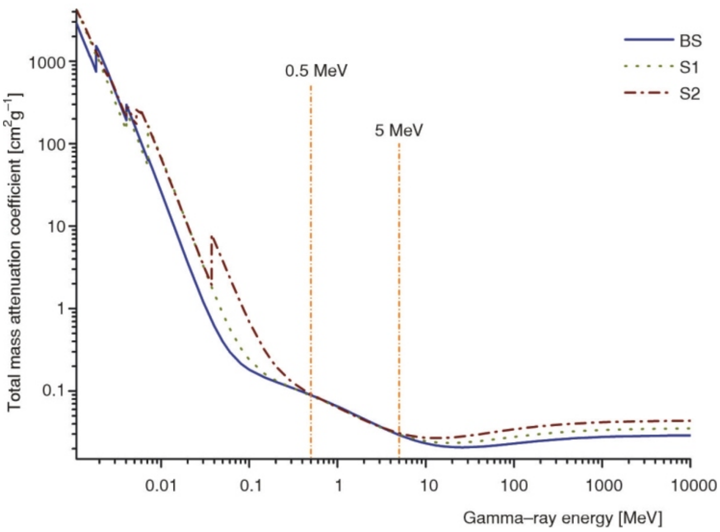

Figure 7. Total mass attenuation coefficients *vs*. gamma-ray energy for three samples

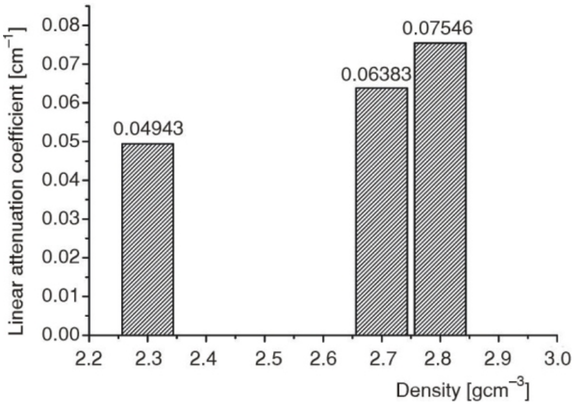

Figure 8. Gamma-ray linear attenuation coefficients for three samples at 15 MeV

showed a 25.4 % more mass attenuation factor than the sample without barite at 15 MeV.

Figure 8 shows the dependences of the theoretically calculated linear attenuation coefficients in the samples at $E_\gamma = 15$ MeV, by using eq. (1). When comparing samples S1 and S2, the linear attenuation coefficients increased by 18 % due to the increase in density values with the addition of barite. In Akkurt *et al*. [32], an increase (16 %) was also found in concrete when the calcite filler was completely replaced with barite filler.

The experimentally found linear attenuation coefficients at $E_\gamma = 15$ MeV for three concrete samples with different contents of B_4C, Fe_3O_4, and $BaSO_4$, tab. 1, are shown in fig. 9.

According to the experimental results, fig. 9, it can be seen that the attenuation of gamma quanta through the material occurs exponentially with the thickness of the absorber. This attenuation obeys the Beer-Lambert law [33] and strongly depends on the density of the shielding material [34]. Figure 10 compares the samples' theoretically calculated linear attenuation coefficients with those obtained from experimental measurements. The figure clearly shows that the differences between the theoretically calculated and experimental linear attenuation coefficients can increase the radiation dose by an average of 4.8 %.

In general, it can be considered that an increase in density of 22 % gives the concrete an increase in the linear attenuation coefficient μ of about 53 %. Based on the obtained measurement results, the mean free path, half- and- tenth-value layers that are the most used

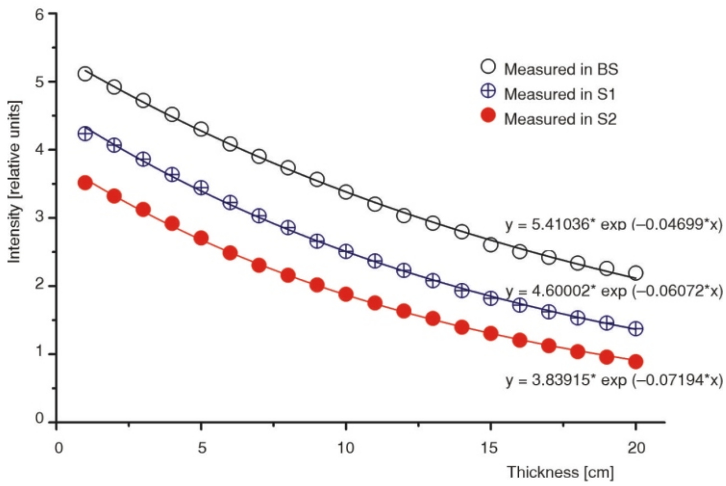

Figure 9. Experimental results of measurements on a linear accelerator with exponential fittings

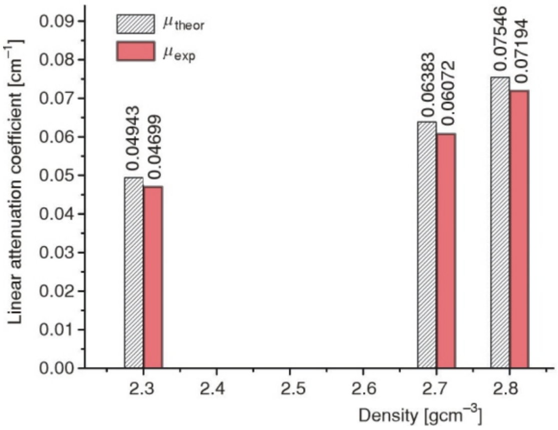

Figure 10. Experimentally obtained and theoretically calculated linear attenuation coefficients at $E_\gamma = 15$ MeV

transmission layers of the gamma rays in shield design were calculated, fig. 11. The attenuation thickness of the samples decreased with the addition of barite.

Compared to conventional concrete, the linear attenuation coefficient for concrete with the highest barite content increased by 53.1 %, and the thickness of the half-value layer decreased by 34.7 %. Therefore, S2 concrete samples can better replace any materials currently used for the construction of nuclear power centers due to their properties and low cost; while concrete and brick are better used for the construction of nuclear medicine diagnostic centers.

CONCLUSION

As a result, experimental linear attenuation coefficients of samples with various impurities were obtained, fig. 10, and it was shown.

good agreement between the experimentally obtained linear coefficients and theoretically calculated values with the XCOM program, which in turn shows the possibility of using the Elekta Axesse accelerator to study materials for future thermonuclear power engineering and nuclear medicine

a good absorber of 15 MeV gamma rays is concrete (S2) with a high content of $BaSO_4$, fig. 11.

Thus, the primary barrier for radiation protection must be made of concrete enriched with heavy material such as barite. At the same time, a comparison of theoretically calculated and experimentally measured linear attenuation coefficients showed differences of 4.8 % on average, which must be considered when using these materials in construction and estimating the expected radiation dose. Such samples should also be studied for radiation resistance from neutron radiation.

ACKNOWLEDGMENT

This research was funded by the Science Committee of the Ministry of Education and Science of the Republic of Kazakhstan (Grant No. AP09058404).

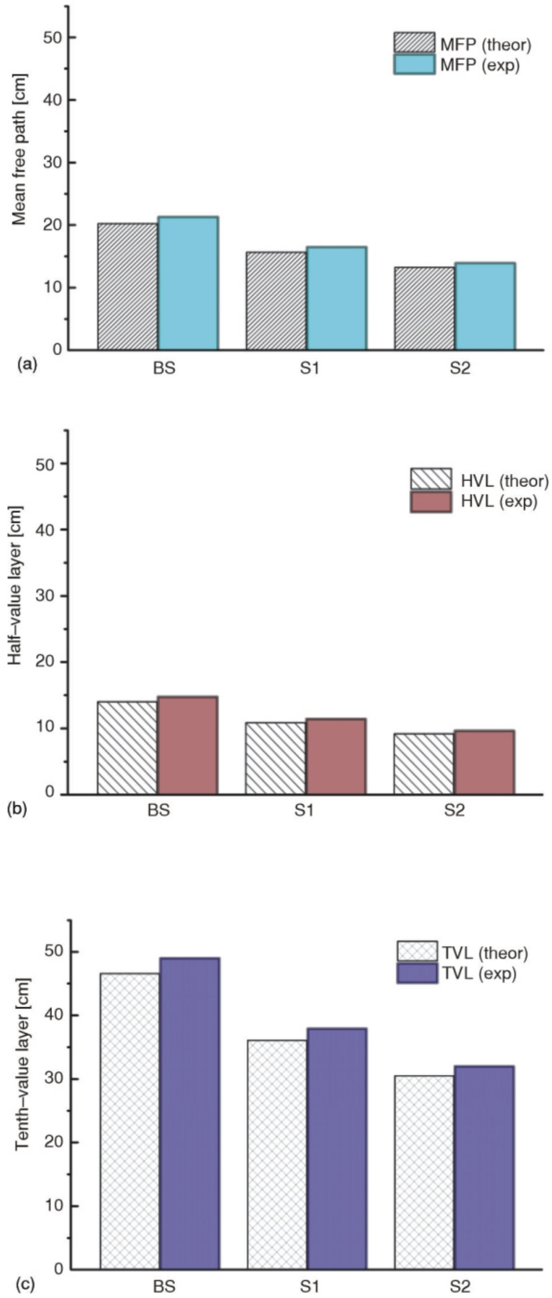

Figure 11. Mean free path (a), half-value layer (b), and tenth-value (c) layer for gamma-ray at 15 MeV

AUTHORS CONTRIBUTIONS

Conceptualization, Y. Zaripova and V. Dyachkov; methodology, T. Gladkikh and N.A.N. Diab; soft-ware, M. Bigeldiyeva and V. Dyachkov; formal analysis, Y. Zaripova, V. Dyachkov and N.A.N. Diab; investigation, Y. Zaripova and T. Gladkikh; re-sources, V. Dyachkov and M. Bigeldiyeva; data curation, Y. Zaripova; writing-original draft preparation, review and editing, Y. Zaripova and V. Dyachkov; visualization, M. Bigeldiyeva; supervision, Y. Zaripova; funding acquisition, Y. Zaripova. All authors have read and agreed to the published version of the manuscript.

REFERENCES

[1] Manohara, S. R., Hanagodimath S. M., Effective Atomic Numbers for Photon Energy Absorption of Essential Amino Acids in the Energy Range 1 keV to 20 MeV, *Nuclear Instruments and Methods in Physics Research Section B, 264* (2007), 1, pp. 9-14

[2] Buyukyildiz, M., Kurudirek, M., Radiological Properties of Healthy, Carcinoma and Equivalent Breast Tissues for Photon and Charged Particle Interactions, *International Journal of Radiation Biology, 94* (2018), 1, pp. 70-78

[3] Biswas, R., *et al*., Calculation of Gamma-Ray Attenuation Parameters for Locally Developed Shielding Material: Polyboron, *Journal of Radiation Research and Applied Sciences, 9* (2016), 1, pp. 26-34

[4] Gulbicim, H., *et al*., The Investigation of Vermiculite as an Alternating Shielding Material for Gamma Rays, *Radiation Physics and Chemistry, 130* (2017), Jan., pp. 112-117

[5] Obaid, S. S., *et al*., Determination of Gam*ma Ray Shielding Parameters of Rocks and Concrete, Radiation Physics and Chemistry, 144* (2018), Mar., pp. 356-360

[6] Yakunin, S., *et al*., Detection of Gamma Photons Using Solution-Grown Single Crystals of Hybrid Lead Halide Perovskites, *Nature Photonics, 10* (2016), pp. 585-589

[7] Sayyed, M. I., *et al.*, Comprehensive Study on Estimation of Gamma-Ray Exposure Buildup Factors for Smart Polymers as a Potent Application in Nuclear Industries, *Results in Physics, 9* (2018), June, pp. 585-592

[8] Lokhande, R. M., *et al*., Determination of Attenuation Parameters and Energy Absorption Build-Up Factor of Amine Group Materials, *Radiation Physics and Chemistry, 141* (2017), Dec., pp. 292-299

[9] Hubbell, J. H., Review of Photon Interaction Cross Section Data in the Medical and Biological Context, *Physics in Medicine & Biology, 44* (1999), 1, R1

[10] Michaelides, E. E., Michaelides, D. N., Impact of Nuclear Energy on Fossil Fuel Substitution, *Nuclear Engineering and Design, 366* (2020), Sept., 110742

[11] Gökçe, H. S., *et al.*, Gamma-Ray Attenuation Coefficients and Transmission Thickness of High Consistency Heavyweight Concrete Containing Mineral Admixture, *Cement and Concrete Composites, 92* (2018), Sept., pp. 56-69

[12] Makarious, A., *et al.*, On the Utilization of Heavy Concrete for Radiation Shielding, *Annals of Nuclear Energy, 23* (1996), 3, pp. 195-206

[13] McCaffrey, J. P., et al., Radiation Attenuation by Lead and Nonlead Materials Used in Radiation Shielding Garments, *Medical Physics, 34* (2007), 2, pp. 530-537

[14] Abbas, Y., *et al*., Gamma Attenuation Through Nano Lead – Nano Copper PVC Composites, *Nucl Technol Radiat, 36* (2021), 1, pp. 50-59

[15] More, C., *et al.*, Extensive Theoretical Study of Gamma-Ray Shielding Parameters Using Epoxy Resin-Metal Chloride Mixtures, *Nucl Technol Radiat., 35* (2020), 2, pp. 138-149

[16] Han, I., Demir, L. Determination of Mass Attenuation Coefficients, Effective Atomic and Electron Numbers for Cr, Fe and Ni Alloys at Different Energies, *Nuclear Instruments and Methods in Physics Research Section B, 267* (2009), 1, pp. 3-8

[17] Elsheikh, N. A. A., Monte Carlo Gamma Transmission Model for Characterization of Multi-Gamma Shielding Parameters of Some Heavy Metal Oxide Glasses, *Nucl Technol Radiat, 36* (2021), 4, pp. 338-345

[18] Ozan Tekin, H., *et al*., Altunsoy E. E., Photon Shielding Characterizations of Bismuth Modified Borate-Silicate-Tellurite Glasses Using MCNPX Monte Carlo code, *Materials Chemistry Physics, 211* (2018), June, pp. 9-16

[19] Agar, O., Study on Gamma Ray Shielding Performance of Concretes Doped with Natural Sepiolite Mineral, *Radiochimica Acta, 106* (2018), 12, pp. 1009-1016

[20] Singh, V. P., *et al*., Investigation on Radiation Shielding Parameters of Ordinary, Heavy and Super Heavy concretes, *Nucl Technol Radiat, 29* (2014), 2, pp. 149-156

[21] Ozyurt, O., *et al*., Calculation of Gamma Ray Attenuation Coefficients of Some Granite Samples Using a Monte Carlo Simulation Code, *Radiation Physics and Chemistry, 144* (2018), Mar., pp. 271-275

[22] Obaid, S. S., *et al*., Determination of Gamma Ray Shielding Parameters of Rocks and Concrete, *Radiation Physics and Chemistry, 144* (2018), Mar., pp. 356-360

[23] Akkurt, I., *et al*., The Properties of Various Igneous Rocks for X-Ray Shielding, *Construction and Building Materials, 21* (2007), 12, pp. 2078-2082

[24] Ali, A. M., Determination of Attenuation Properties for Some Building Materials by MCNP Simulation, *Arab Journal of Nuclear Sciences and Applications, 48* (2015), 1, pp. 33-39

[25] ***, Stereotactic Radiation Therapy Elekta Axesse. Guide to Using the system, UK, 2008, p. 104

[26] Chugunov, I. N., *et al*., Development of Gamma-Ray Diagnostics for ITER, *Nuclear Fusion, 51* (2011), 8, 083010

[27] Mack, J. M., *et al*., Remarks on Detecting High-Energy Deuterium--Tritium Fusion Gamma Rays Using a Gas Cherenkov Detector, *Radiation Physics and Chemistry, 75* (2006), 5, pp. 551-556

[28] Polaczek-Grelik, K., *et al*., *Gamma Radiation in the Vicinity of the Entrance to Linac Radiotherapy Room*, IntechOpen, London, UK, 2019, p. 260

[29] Zaripova, Yu. A., *et al*., Application of the Medical Linear Accelerator ELEKTA AXESSE in the Study of Sorption Properties of Impurities and Absorption Coefficients of Medium and Heavy Chemical Elements, *Journal of Physics: Conference Series, 2155* (2022), 1, 012029

[30] Berger, M. J., *et al*., XCOM: Photon Cross Sections Database. Available online: https://dx.doi.org/10.18434/T48G6X (accessed on 04 July 2023)

[31] Knoll, G. F., *Radiation Detection and Measurement*, 3rd ed., John Wiley and Sons Inc., New York, USA, 1999, p. 802

[32] Akkurt, I., *et al*., Photon Attenuation Coefficients of Concrete Includes Barite in Different Rate, *Annals of Nuclear Energy, 37* (2010), 7, pp. 910-914

[33] Kazjonovs, J., *et al*., Designing of High Density Concrete by Using Steel Treatment Waste, *Proceedings*, 10th Int. Conf. Mod. Build. Mater. Struct. Tech., Vilnius, Lithuania, 2010, pp. 138-142

[34] Gonzalez-Ortega, M. A., *et al*., Radiological Protection and Mechanical Properties of Concretes with EAF Steel Slags, *Construction and Building Materials, 51* (2014), Jan., pp. 432-438

Received on July 14, 2023
Accepted on October 11, 2023

Јулија ЗАРИПОВА, Вјачеслав ДЈАЧКОВ, Татјана ГЛАДКИХ, Миргул БИГЕЛДИЈЕВА, Наср Ахмед Наср ДИАБ

ИСТРАЖИВАЊЕ СВОЈСТАВА ЗАШТИТЕ ОД ГАМА ЗРАЧЕЊА МОДИФИКОВАНИХ КОНСТРУКТИВНИХ МАТЕРИЈАЛА ЗА НУКЛЕАРНУ ЕНЕРГЕТИКУ И НУКЛЕАРНУ МЕДИЦИНУ

У овом раду испитиване су карактеристике заштите три узорка бетона са различитим садржајима B_4C, Fe_3O_4 и $BaSO_4$, одређивањем њихових теоријских и експерименталних масених коефицијената слабљења при енергијама фотона од 15 MeV. Масени коефицијенти слабљења $_m$ теоретски су израчунати XCOM програмом коришћењем хемијског састава узорака. Затим су линеарни коефицијенти слабљења μ израчунати познавањем вредности μ_m. Elekta Axesse акцелератор коришћен је за експериментално одређивање линеарних коефицијената слабљења узорака са различитим примесама. Вредности μ од 0.4699 cm^{-1}, 0.6072 cm^{-1} и 0.7194 cm^{-1} добијене су на 15 MeV, за узорак без примеса, узорак са магнетитом и узорак са баритом, респективно. Резултати су упоређени са коефицијентима добијеним XCOM програмом и показали су добру сагласност између две методе. Линеарни коефицијент слабљења употребљен је да се израчунају слојеви који слабе зрачење два и десет пута. У поређењу са конвенционалним бетоном, линеарни коефицијент слабљења бетона са највећим садржајем барита повећан је за 53.1 %, а дебљина слоја полуслабљења смањена је за 34.7 %. Такав узорак може се користити као грађевински материјал за медицинске центре и нуклеарне електране.

Кључне речи: бетон, заштита од зрачења, линеарни коефицијент слабљења, слој полуслабљења